THERMAL CONVECTION IN A POROUS MEDIUM
WITH CONTINUOUS PERIODIC STRATIFICATION

by

Kjell M. Gjerde and Peder A. Tyvand
Department of Mechanics, University of Oslo
Norway

Abstract - The onset of convection in a horizontal stratified porous layer heated form below is studied theoretically. The stratification is continuous and periodic, with $N/2$ periods within the layer. For large numbers of N the critical Rayleigh number converges towards the limit of homogeneous anisotropy with a deviation proportional to N^{-2}.

NOMENCLATURE

- a — coefficient in the permeability distribution (21), parameter in the series expansion (32);
- C — factor of proportionality in eq. (30);
- c_p — specific heat at constant pressure;
- D — $= d/dz$;
- E — relative difference between numerical and analytical results for R_c;
- f — dimensionless inverse permeability, $K_v/K(z)$;
- g — acceleration of gravity;
- h — depth of porous medium;

$K(z)$ permeability distributions;

K_1, K_2 permeabilities of the two layers in the discrete model [5-7];

K_H, K_V effective horizontal and vertical permeabilities;

$\vec{k}$ vertical unit vector;

k, l dimensionless wave numbers;

L dimensionless cell width, π/α;

L_c preferred cell width, giving $R = R_{c\ min}$;

$L_c^{(aniso)}$ preferred cell width for homogeneous anisotropy, $\xi^{1/4}$;

N number of layers in the discrete model [5-7], here twice the number of periods in the permeability distribution;

p pressure;

R^* Rayleigh number, $K_V g \gamma h \Delta T/(\kappa_m \nu)$;

R redefined Rayleigh number, $R^*/(4\pi^2)$;

R_c critical Rayleigh number, given by $\sigma = 0$;

$R_c^{(aniso)}$ critical Rayleigh number for homogeneous anisotropy;

$R_{c\ min}$ Rayleigh number at onset of convection, given by $d(R_c)/dL = 0$;

T dimensionless temperature;

ΔT temperature difference between lower and upper boundary;

t dimensionless time;

$\vec{v}$ dimensionless velocity;

W z-dependent part of w;

w dimensionless vertical velocity, $\vec{v} \cdot \vec{k}$;

x, y, z cartesian coordinates.

GREEK SYMBOLS

α dimensionless overall wave number, $(k^2+l^2)^{\frac{1}{2}}$;

β layering parameter in the discrete model [5-7], K_2/K_1;

γ coefficient of volume expansion;

Θ z-dependent part of θ;

θ dimensionless temperature perturbation;

κ_m thermal diffusivity of saturated porous medium;

λ_m thermal conductivity of the saturated porous medium;

ν kinematic viscosity;

ξ anisotropy parameter, K_H/K_V;

$\zeta^{(trunc)}$ anisotropy parameter for a truncation of Fourier series (20);

ρ density.

1. INTRODUCTION

The present paper is a contribution to the theory of free thermal convection in inhomogeneous porous media. We will first place it in a context of previous work.

Masuoka et al. [1] studied thermal convection in a porous medium composed of two layers of different permeabilities or thermal conductivities. Earlier Gheorghitza [2] had treated this problem for weak permeability contrast. McKibbin & O'Sullivan [3] presented a general method of analyzing the onset of convection in a porous medium composed of discrete, homogeneous layers. In their second paper [4] they made a corresponding analysis of the heat transport at slightly supercritical Rayleigh numbers. Only the cases of two and three layers were investigated in these papers. McKibbin & Tyvand [5-7] applied these methods to thermal convection in multilayered porous media composed of alternating layers, which are suited for a comparison with homogeneous anisotropy [8].

McKibbin & Tyvand [5-7] investigated only configurations with a number of layers of order 10 or less, because the treatment of the internal boundary conditions requires much computer capacity.

In the present paper the corresponding problem of continuous stratification is considered. This is simpler than the discrete case from a mathematical point of view, as internal boundary conditions are avoided. Thereby numbers of strata up to the order of 100 are tractable numerically. This enables us to perform a thorough investigation of the asymptotic convergence towards homogeneous anisotropy. The numerical results are confirmed by analytical results, where a series expansion valid for small variations in permeability is applied.

Among earlier works on convection in porous media with continuous permeability variation, we mention Gheorghitza [2] and Ribando & Torrance [9]. These authors studied monotonic permeability variations, in contrast to the periodic variation to be considered here.

2. MATHEMATICAL FORMULATION

We consider an isotropic porous medium with permeability $K(z)$ confined between two horizontal planes $z = 0$ and $z = h$. z is the vertical coordinate. Average horizontal and vertical permeabilities are defined by [10, p.157]:

$$K_H = h^{-1} \int_0^h K(z)dz \tag{1}$$

$$K_v = h\left(\int_0^h \frac{dz}{K(z)}\right)^{-1} \tag{2}$$

We introduce the ratio of effective anisotropy:

$$\xi = K_H/K_v \tag{3}$$

From Schwartz' inequality it is readily proved that $\xi \geq 1$, with the equality sign reserved for the case of constant permeability. We introduce a notation for the dimensionless inverse permeability:

$$f(z) = K_v/K(z) \tag{4}$$

The fluid-filled porous medium is assumed to have a constant thermal conductivity λ_m. Its thermal diffusivity is given by [11]

$$\kappa_m = \lambda_m/(c_p\rho)_f \tag{5}$$

where c_p is the specific heat at constant pressure and ρ the density. The subscripts f and m refer to the saturating fluid and the porous medium (mixture of solid and fluid), respectively. By choosing

$$h,\ (c_p\rho)_m h^2/\lambda_m,\ \kappa_m/h,\ \Delta T,\ \rho\nu\kappa/K_v \tag{6}$$

as units of dimensionless length, time, velocity, temperature and pressure, we get the dimensionless equations for buoyancy-driven convection;

$$f\vec{v} + \nabla p - R^{*}T\vec{k} = 0 \tag{7}$$

$$\nabla\cdot\vec{v} = 0 \tag{8}$$

$$\frac{\partial T}{\partial t} + \vec{v}\cdot\nabla T = \nabla^2 T \tag{9}$$

valid in the standard Darcy-Boussinesq-approximation. The Rayleigh number R^{*} is defined by:

$$R^{*} = \frac{K_v g\gamma h\Delta T}{\kappa_m \nu} \tag{10}$$

The layer is heated form below with a temperature difference ΔT between the boundaries. The dimensionless temperature field is written;

$$T = T_0/\Delta T - z + \theta \tag{11}$$

where θ denotes the deviation from the conduction solution. The requirements of impermeable, perfectly conducting boundaries may then be expressed as:

$$w = \theta = 0 \quad \text{at} \quad z = 0,1 \tag{12}$$

The convective term in the heat equation (9) is linearized, and a horizontal Fourier component is considered:

$$w = W(z)\exp[i(kx+ly) + \sigma t] \tag{13}$$

$$\theta = \Theta(z)\exp[i(kx+ly) + \sigma t] \tag{14}$$

From eqs. (9)-(11) we then get:

$$f(D^2-\alpha^2)W + f'DW = -\alpha^2 R^* \Theta \tag{15}$$

$$W = (\sigma - D^2+\alpha^2)\Theta \tag{16}$$

with boundary conditions

$$W = \Theta = 0, \; z = 0,1 \tag{17}$$

In (15)-(16) we have introduced the notation

$$D = d/dz \tag{18}$$

and the overall wave number

$$\alpha = (k^2+l^2)^{\frac{1}{2}} \tag{19}$$

The eigenvalue problem (15)-(17) is solved numerically by the shooting method [12, p.142]. For given α and R, the eigenvalue σ may be found by one integration from $z = 0$ to $z = 1$. The boundary value problem ((15)-(17) is self-adjoint [13, p.53]. Then σ is real and marginal stability is given by $\sigma = 0$. A Newton-Raphson iteration procedure determines the value of R giving $\sigma = 0$ for each chosen value of α. By putting $\sigma = 0$, R may be considered as eigenvalue in the problem. We will find only the solution with the lowest eigenvalue for R, being the physically preferred solution. This is achieved by starting the iteration with values of R close to the lowest eigenvalue for homogeneous anisotropy.

In their first study, McKibbin and Tyvand [5] concentrated on N alternating layers of equal thicknesses and permeabilities K_1 and βK_1. The Fourier series of that distribution is (with respect to inverse permeability):

$$\frac{K_1^{-1}+\beta K_1^{-1}}{2} + \frac{2}{\pi}(K_1^{-1} - \beta K_1^{-1}) \sum_{n=1}^{\infty} \frac{\sin(2n-1)N\pi z}{2n-1} \tag{20}$$

This series converges slowly and is not suited as a direct representation of the discrete model.

In the present paper we consider a continuous periodic permeability distribution given by

$$f = 1 + a \sin N\pi z \tag{21}$$

This corresponds to truncating the series in (20) after one term only. The number of periods of permebility variation is $N/2$. We consider only even numbers for N, so that only complete periods are present within the boundaries. Then the effective anisotropy parameter attached to the permeability distribution (21) is

$$\xi = (1-a^2)^{-\frac{1}{2}} \tag{22}$$

The effective anisotropy parameter for the discrete model of McKibbin & Tyvand [5], represented here by the full Fourier series (20) is

$$\xi = \tfrac{1}{4}(1+\beta)(1+\beta^{-1}) \tag{23}$$

By interpreting (21) as a truncation of (20) we determine a value for a:

$$a = \frac{4}{\pi}\,\frac{1-\beta}{1+\beta} \tag{24}$$

Through (22) this gives an effective anisotropy parameter for the truncated Fourier series:

$$\xi^{(trunc)} = (1 - \frac{16}{\pi^2} \frac{(1-\beta)^2}{(1+\beta)^2})^{-\frac{1}{2}} \tag{25}$$

In fig. 1 the anisotropy parameters ξ and $\xi^{(trunc)}$ are displayed as functions of β. The curves are symmetric about $\beta=1$ in the log-log diagram. We have two intersection points given by $\beta = 0.24$ and $\beta = 4.2$, where $\xi = \xi^{(trunc)} = 1.609$. In the regions $0.24 < \beta < 1$ and $1 < \beta < 4.2$ we find that $\xi^{(trunc)}$ is slightly below ξ. Outside these regions $\xi^{(trunc)}$ may become much larger than ξ. There are vertical asymptotes for $\xi^{(trunc)}$ at $\beta_{min} = 0.120$ and $\beta_{max} = 8.32$. $\xi^{(trunc)}$ does not exist for $\beta < \beta_{min}$ or $\beta > \beta_{max}$. This is because the one-term truncation of the Fourier series (20) in meaningless when it corresponds to regions of negative permeability. At $\beta = \beta_{min}$ and $\beta = \beta_{max}$ the value of ξ is 2.606. Accordingly, a representation of a given discrete layering by a one-term truncation of its Fourier series is relevant only for small effective anisotropy.

As a supplement to the numerical computations, we will also give analytical results in terms of series expansions with respect to the parameter a introduced in (21). These results are valid only for small values of a, i.e. for ξ of order one, cf. (22). Eq. (22) may be expanded in powers of a;

$$\xi = 1 + \frac{1}{2}a^2 + \frac{1 \cdot 3}{2 \cdot 4}a^4 + \frac{1 \cdot 3 \cdot 5}{2 \cdot 4 \cdot 6}a^6 + \ldots \tag{26}$$

relevant to the discussion in chapter 4.

3. NUMERICAL RESULTS

In the presentation of the results we will apply a Rayleigh number R defined by

$$R = \frac{R^*}{4\pi^2} \tag{27}$$

so that the onset of convection in the classical Lapwood problem [14,15] occurs for $R = 1$. We will investigate the critical Rayleigh number R_c at marginal stability ($\sigma = 0$) as a function of the dimensionless cell width $L(= \pi/\alpha)$. The convergence towards homogeneous anisotropy as N increases will be studied in detail.

From Kvervold & Tyvand [8] we quote the critical Rayleigh number for a layer with homogeneous anisotropic permeability

$$R_c^{(aniso)} = \frac{(\xi\alpha^2+\pi)(\alpha^2+\pi^2)}{4\pi^2\xi\alpha^2} = \frac{(\xi+L^2)(1+L^2)}{4\xi L^2} \tag{28}$$

with a minimum value

$$R_{c\ min}^{(aniso)} = \frac{1}{4}(1 + \xi^{-\frac{1}{2}})^2 \tag{29}$$

corresponding to the preferred cell width

$$L_c^{(aniso)} = \xi^{1/4} \tag{30}$$

In fig. 2 some numerical results for R_c as a function of L are displayed. Fig. 2(a),(b) and (c) represent $\xi = 2.294$, $\xi = 7.089$ and $\xi = 25.005$, respectively. These figures show a convergence towards homogeneous anisotropy as N increases.

Above we have linked the comparison with the discrete model [5-7] to a truncation of its Fourier series. However, one might argue that a better way of comparison is by equal values of ξ. To compare with the present fig. 2, (a) & (b) we then have figs.1 & 3 in [5]. Those figures show results for alternating discrete layers of equal thicknesses with effective anisotropy given by $\xi = 2.0$ and $\xi = 25.5$, respectively.

Characteristic for the discrete models in [5] and [6] where the thinner layer is not the more permeable one, is the possibility of local convection. Local convection takes place when a local Rayleigh number (with respect to a single layer) reaches its critical value before the whole layered system becomes unstable to large-scale disturbances. Local convection mainly consists of recirculations within single layers. It is characterized <u>both</u> by a small preferred cell width ($L_c < 1$) and a corresponding critical Rayleigh number below the value for homogeneous anisotropy.

In the case of a very permeable thinner layer [7] no local convection is found. The preferred cell width is always relatively large ($L_c > 1$) and the critical Rayleigh number is mostly above the value for homogeneous anisotropy.

Also in the present continuous model truely local convection is absent. Only for $N = 2$ we find a small preferred cell width ($L_c < 1$). But the corresponding critical Rayleigh numbers are always above the values for homogeneous anisotropy. One reason for the absence of local convection is that there is no clear notion of individual layers in which recirculation might take place. So the influence (due to continuity) of passive regions of low permeability is much stronger than in the discrete case. Returning to the Fourier series (20) we have now found that a one-term truncation has a significant physical effect; to remove the possibility of local convection.

The derivation of R_c from homogeneous anisotropy is much less dependent on ξ than in the discrete case. This is related to the fact that local convection is absent, and will be discussed further in connection with fig. 3 below.

The preferred cell width L_c giving minimum value $R_{c\ min}$ at marginal stability has been investigated. Some of the results are shown in table 1. For $N = 2$ it differs much from $L_c^{(aniso)}$, and this case is not included in the table. But already for $N = 4$, L_c is relatively close to $L_c^{(aniso)}$. For $N > 6$ no difference between $R_c(L_c^{(aniso)})$ and $R_{c\ min}$ are detectable within our accuracy of computation.

	N	4	6	8	10
$\xi = 2.294$, $L_c^{(aniso)} = 1.231$	L_c	1.207	1.225	1.228	1.230
	$R_{c\ min}$	0.7416	0.7160	0.7049	0.6993
	$R_c(L_c^{(aniso)})$	0.7418	0.7160	0.7049	0.6993

	N	4	6
$\xi = 25.005$, $L_c^{(aniso)} = 2.236$	L_c	2.206	2.235
	$R_{c\ min}$	0.4477	0.3986
	$R_c(L_c^{(aniso)})$	0.4478	0.3986

Table 1. Some results for the critical cell width L_c, the corresponding Rayleigh number $R_{c\ min}$ and the value of R_c corresponding to critical cell width for homogeneous anisotropy.

In fig. 3 the convergence of R_c towards $R_c^{(aniso)}$ is displayed in a log-log diagram. For different values for N, the deviation $R_c - R_c^{(aniso)}$ is marked. For ξ the three values 2.294, 7.089 and 25.005 are chosen.

In fig. 3(a) we have chosen the cell width $L = L_c^{(aniso)}$. Only for $N = 2$ this causes a significant difference between R_c and $R_{c\ min}$. So for $N > 4$ the points represent the onset of convection given by $R_{c\ min}$. Each of the three series of numerical data has a slope with angle coefficient very close to -2, except for some "stochastic" deviations present for $N > 60$. These are due to inadequate convergence of the shooting method, and are very sensitive to the way the Newton-Raphson iteration is terminated.

In fig. 3(b) similar results are shown for $L = 1.7\ L_c^{(aniso)}$. The error tolerance applied in the shooting method is larger here than in fig. 4. Therefore results are displayed only up to N=40.

The same angle coefficient -2 for the numerical data is found here.

We conclude that for $N >> 1$ we have with good accuracy;

$$R_c - R_c^{(aniso)} = \frac{C}{N^2} \tag{31}$$

where the factor of proportionality C is a function of L and of ξ (or a). The ξ-dependence is only slight for large values of ξ. It is more pronounced for small values of ξ, see eq. (36).

The nice asymptotic power law (31) is not likely to be significantly dependent on our choice of $K(z)$ and probably applies to discrete layering [5-7] as well. The results for large-scale convection in those papers are compatible with this conjecture. An odd power dependence of N is prohibited both in the discrete and continuous models, because the physical problem is conserved under the transformation

$$N \rightarrow -N \tag{32}$$

provided N is an even number.

4. ANALYTICAL RESULTS

When a is relatively small, the eigenvalue problem (15)-(17) may be expanded in powers of a. Hereby we write

$$\left.\begin{aligned} W(z) &= \sum_{n=0}^{\infty} a^n W_n(z) \\ \Theta(z) &= \sum_{n=0}^{\infty} a^n \Theta_n(z) \end{aligned}\right\} \tag{33}$$

The physical problem is conserved under the transformation

$$a \rightarrow -a \tag{34}$$

implying that only even powers of a are represented in the expansions.

For $N > 4$ the critical Rayleigh number is found to be:

$$R_c = \frac{\pi^2+\alpha^2}{4\alpha^2}\{\frac{\alpha^2}{\pi^2} + 1 - \frac{a^2}{2} + \frac{a^2}{2N^2}\frac{\alpha^2}{\pi^2}(3 - \frac{\alpha^2}{\pi^2})\}$$
$$+ O(a^2,N^{-4}) + O(a^4,N^0) \qquad (35)$$

From a physical point of view it is clear that the sum of all terms independent of N in the series expansions must correspond to homogeneous anisotropy. The terms independent of N in the complete expansion for R_c will then have as their sum $R_c^{(aniso)}$, given by (28). By adding these terms to the expression (35) we find the improved result:

$$R_c = \frac{\pi^2+\alpha^2}{4\alpha^2}\{\frac{\alpha^2}{\pi^2} + \xi^{-1} + \frac{a^2}{2N^2}\frac{\alpha^2}{\pi^2}(3 - \frac{\alpha^2}{\pi^2})\}$$
$$+ O(a^2,N^{-4}) + O(a^4,N^{-2}) \qquad (36)$$

In (35) the first two terms in the expansion for ξ^{-1} were included, cf. eq. (26).

From (36) it is clear that the factor of proportionality C defined in eq. (31) is a quadratic function of a for weak effective anisotropy ($a \ll 1$). By (22) we find that C is then a linear function of ξ.

A minimization of (36) with respect to α may produce the Rayleigh number at onset of convection. More interesting is the result for the corresponding preferred cell width L_c. Its deviation from homogeneous anisotropy is given by:

$$L_c - L_c^{(aniso)} = \frac{1}{16}\frac{a^4}{N^2} + O(a^4,N^{-4}) + O(a^6,N^{-2}) \qquad (37)$$

From the considerations above it might have been conjectured that the leading term in this deviation would have been of order (a^2,N^{-2}). But the correct result is that it is of order (a^4,N^{-2}), showing the necessity of a quantitative analysis.

We have earlier found the asymptotic power law (31) for $R_c - R_c^{(aniso)}$. This has now been confirmed analytically for weak effective anosotropy. In addition a similar law has been found for $L_c - L_c^{(aniso)}$, which we were not able to find numerically.

In table 2 a quantitative comparison between numerical and analytical results is performed. This gives us some idea of the validity of the series expansion (33). All results are given for $L = L_c^{(aniso)}$. The symbol E denotes the relative amount by which the numerical results for R_c exceed the analytical result (36). We conclude that the series expansions are useful at least in the interval $0 < a < 0.8$.

a	0.2	0.4	0.8	0.9	0.99	
ξ	0.05	1.09	1.67	2.29	7.09	
	0.05	0.25	2.08	3.80	9.56	(N=4)
E	0.04	0.20	1.32	2.23	5.00	(N=6)
	0.03	0.13	0.83	1.36	2.90	(N=8)

Table 2. Comparison between numerical an analytical results for the critical Rayleigh number at $L = L_c^{(aniso)}$.

$$E = \frac{R_c^{(numerical)} - R_c^{(analytical)}}{R_c^{(numerical)}} \times 100\%,$$

where $R_c^{(analytical)}$ is given by eq. (36).

5. SUMMARY

A numerical and analytical study of the marginal stability in a horizontal porous layer heated from below has been performed. The porous medium is periodically stratified, with a sinusoidal variation of the inverse permeability. The basic difference from the corresponding problem of discrete layering is that local convection never occurs in our model. We have found power laws for the deviation from homogeneous anisotropy with respect to critical Rayleigh number and preferred cell width. Good agreement between numerical and analytical results has been found.

REFERENCES

1. T. Masuoka, T. Katsuhara, Y. Nakazono and S. Isozaki, Onset of convection and flow patterns in a porous layer of two different media, Heat Transfer - Japanese Res. 7, 39-52 (1978).

2. St.I. Gheorghitza, The marginal stability in porous inhomogeneous media, Proc.Camb.Phil.Soc. 57, 871-877 (1961).

3. R. McKibbin and M.J. O'Sullivan, Onset of convection in a layered porous medium heated from below, J.Fluid Mech. 96, 375-383 (1980).

4. R. McKibbin and M.J. O'Sullivan, Heat transfer in a layered porous medium heated from below, J.Fluid Mech. 111, 141-173 (1981).

5. R. McKibbin and P.A. Tyvand, Anisotropic modelling of thermal convection in multilayered porous media, J.Fluid Mech. 118, 315-339 (1982).

6. R. McKibbin and P.A. Tyvand, Thermal convection in a porous medium composed of alternating thick and thin layers, Int.J. Heat Mass Transfer, 26, 761-780 (1983).

7. R. McKibbin and P.A. Tyvand, Thermal convection in a porous medium with horizontal cracks. Submitted to Int.J. Heat Mass Transfer (1983).

8. O. Kvernvold and P.A. Tyvand, Nonlinear thermal convection in anisotropic porous media, J.Fluid Mech. 90, 609-624 (1979).

9. R. Ribando and K.E. Torrance, Natural convection in a porous medium; effects of confinement, variable permeability, and thermal boundary conditions. Trans.A.S.M.E.C, J.Heat Transfer 98, 42-48 (1976).

10. J. Bear, Dynamics of Fluids in Porous Media. Elsevier, New York (1972).

11. Y. Katto and T. Masuoka, Criterion for the onset of convective flow in a fluid in a porous medium. Int.J. Heat Mass Transfer 10, 297-309 (1967).

12. H.B. Keller, Numerical Methods for Two-Point Boundary-Value Problems. Blaisdell, Waltham (Mass.) (1968).

13. E. Palm, Nonlinear thermal convection. Ann.Rev. Fluid Mech. 7, 39-61 (1975).

14. C.W. Horton and F.T. Rogers, Convection currents in a porous medium, J.Appl.Phys. 16, 367-370 (1945).

15. E.R. Lapwood, Convection of a fluid in a porous medium. Proc. Camb.Phil.Soc. 44, 508-521 (1948).

FIGURE LEGENDS

Fig. 1 Effective anisotropy as a function of the layering parameter β. Dashed curve represents $\xi^{(trunc)}$. Dashed and dotted lines represent asymptotes for $\xi^{(trunc)}$, given by $\beta = 0.120$ and $\beta = 8.32$.

Fig. 2 Variation of critical Rayleigh number R_c with cell width L for $N = 2,4,6,8,10$ and for an equivalent homogeneous anisotropic layer. (a) $a = 0.9$, $\xi = 2.294$; (b) $a = 0.99$, $\xi = 7.089$; (c) $a = 0.9992$, $\xi = 25.005$.

Fig. 3 Numerical data series for $R_c - R_c^{(aniso)}$ as functions of N. Crosses represent $\xi = 2.294$. Circles represent $\xi = 7.089$. Squares represent $\xi = 25.005$. Triangle represents coinciding circle and square. (a) $L = L_c^{(aniso)}$. (b) $L = 1.7\ L_c^{(aniso)}$.

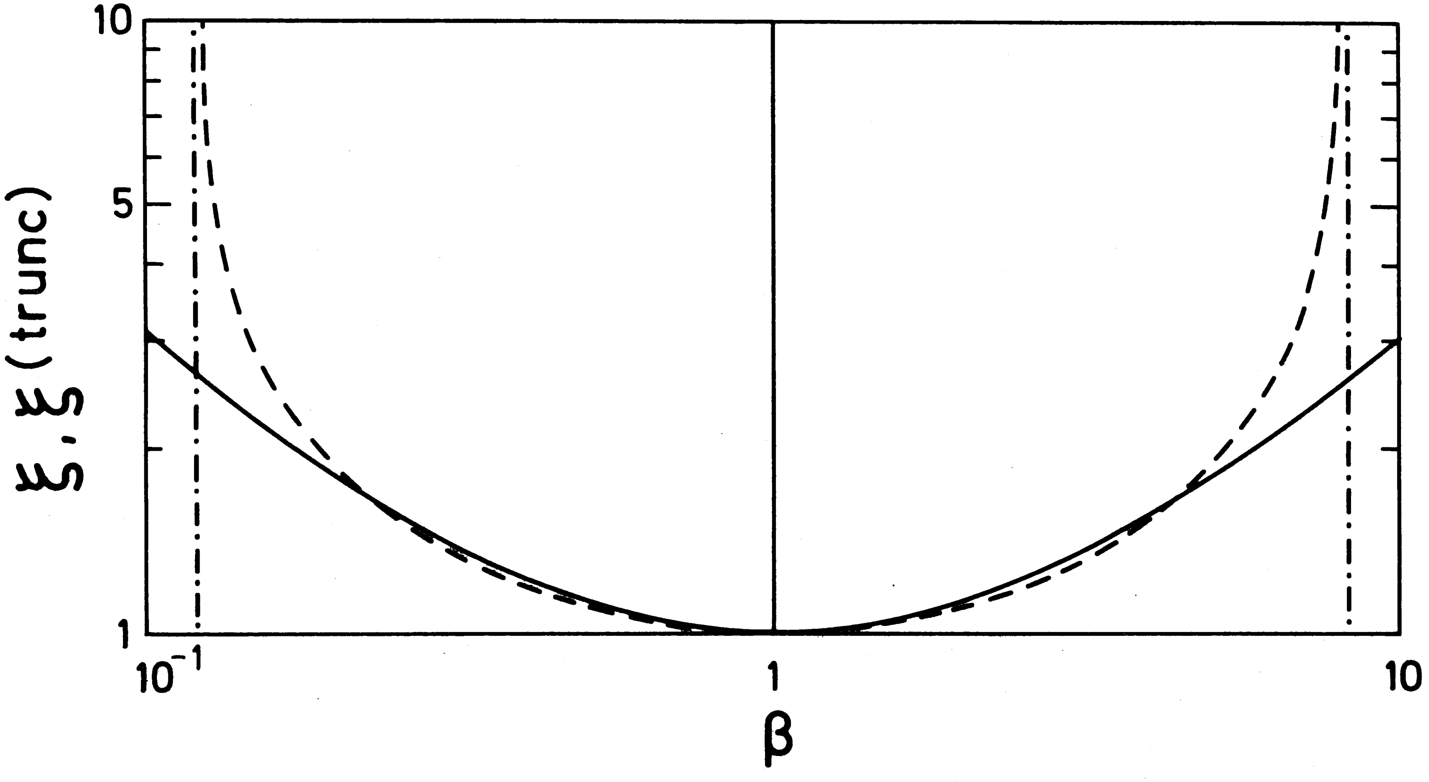

Fig. 1.

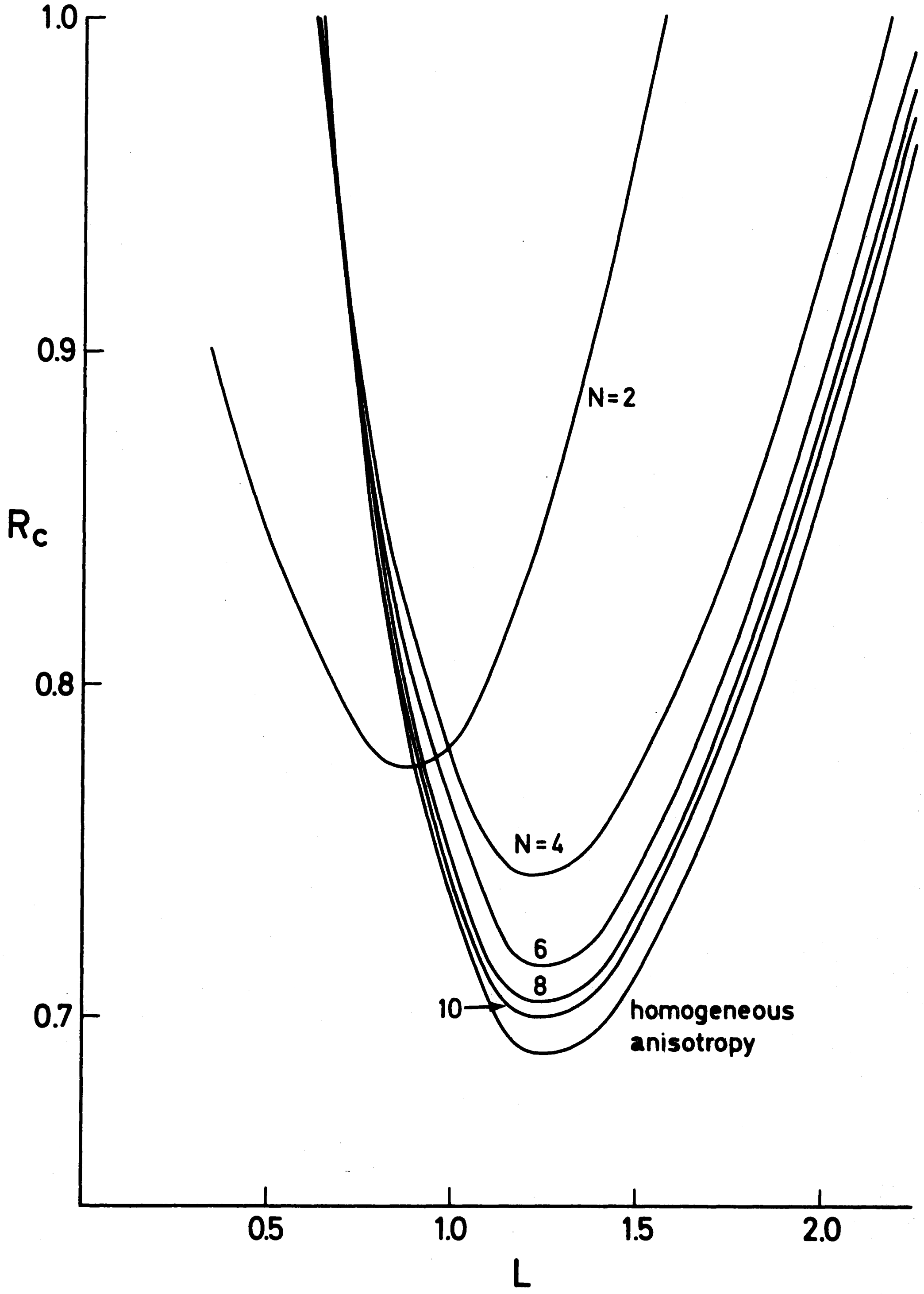

Fig. 2(a).

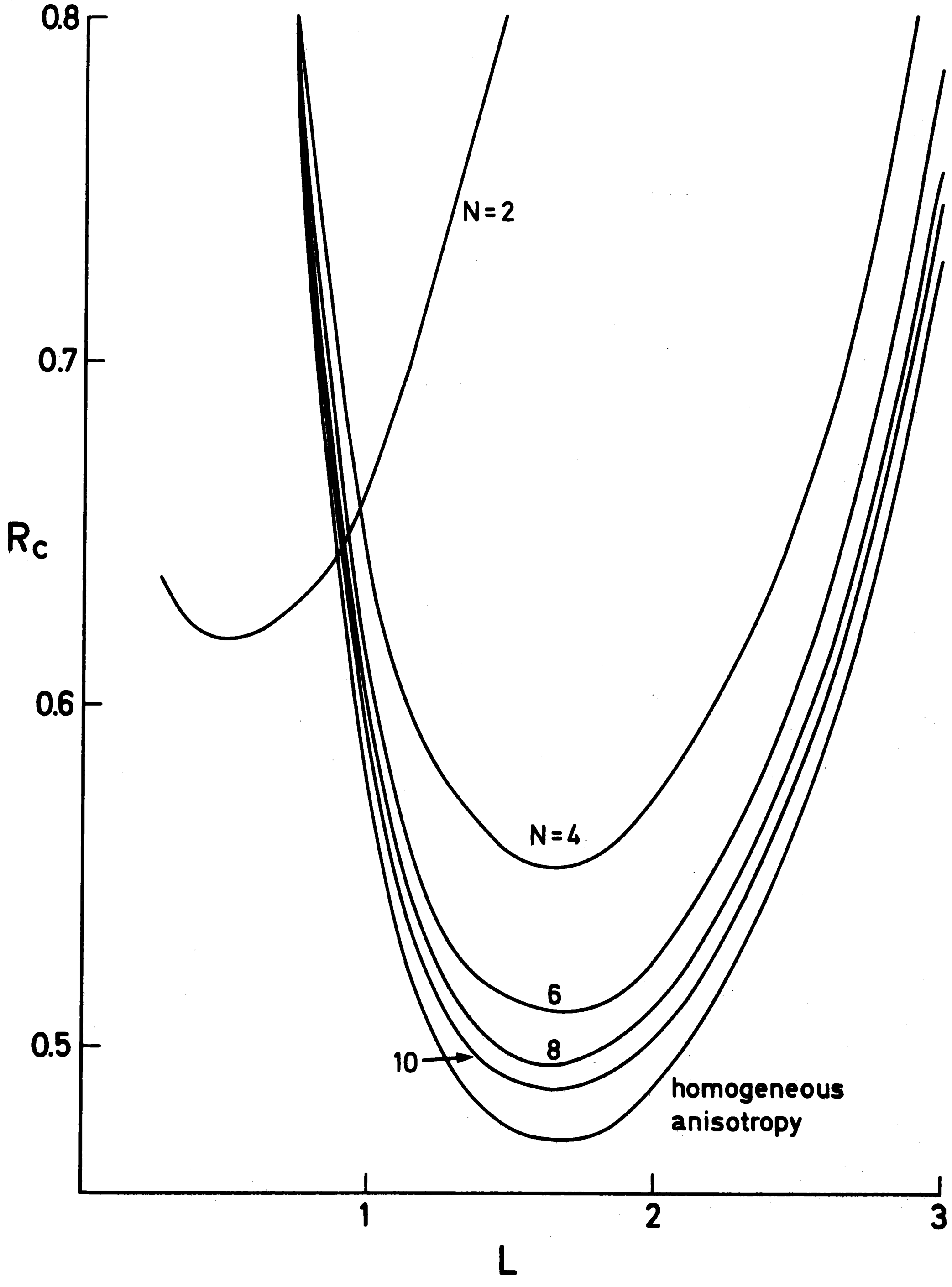

Fig. 2(b).

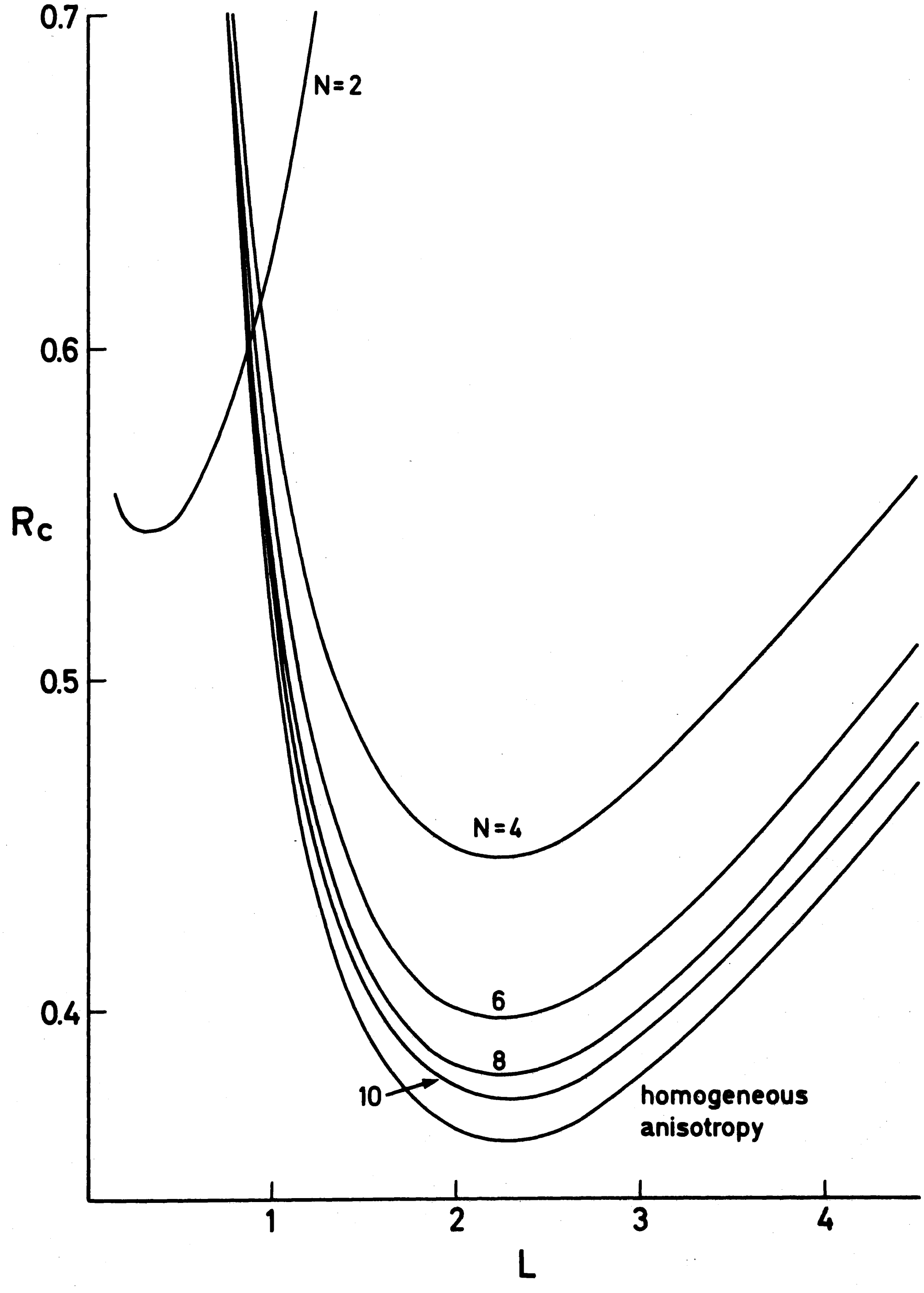

Fig. 2(c).

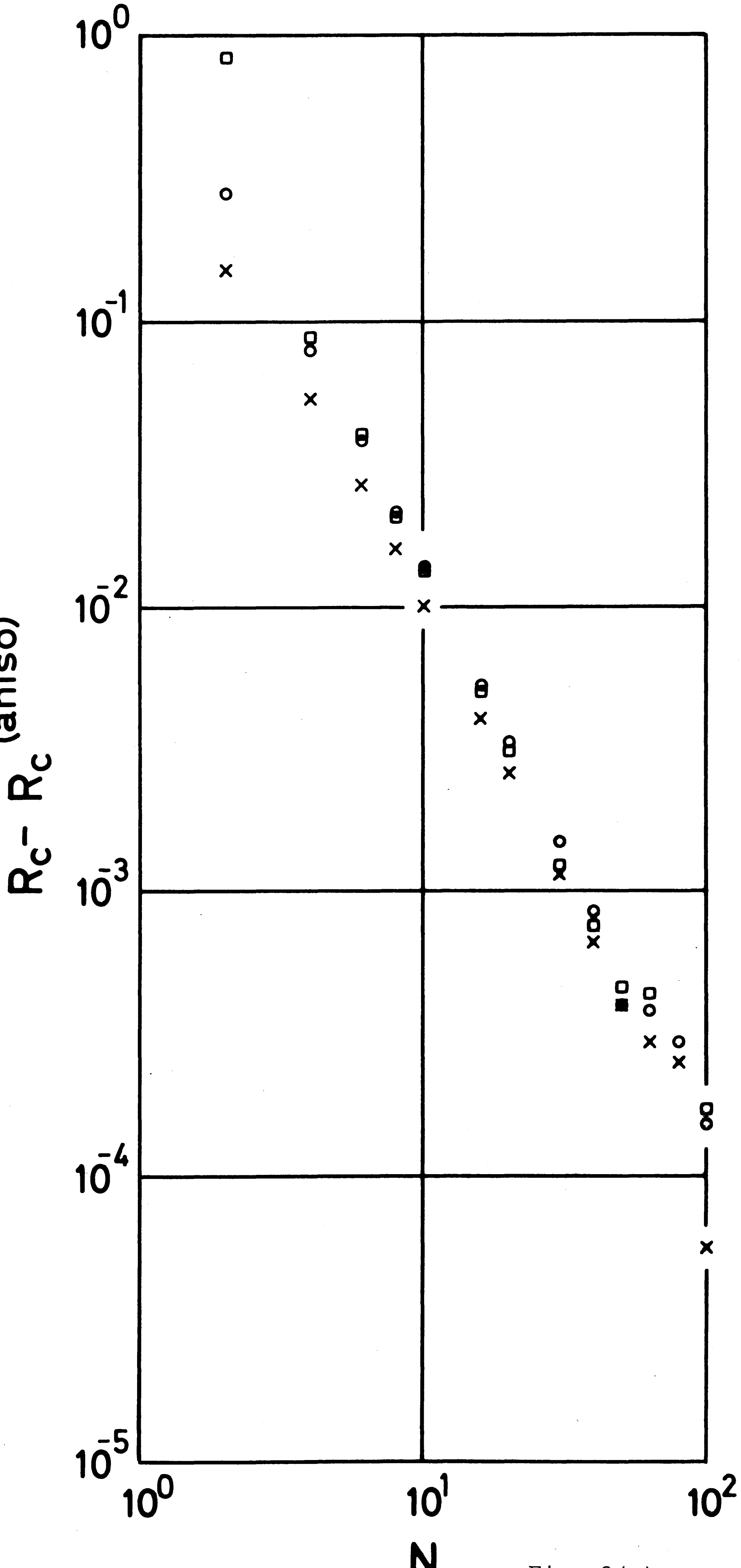

Fig. 3(a).

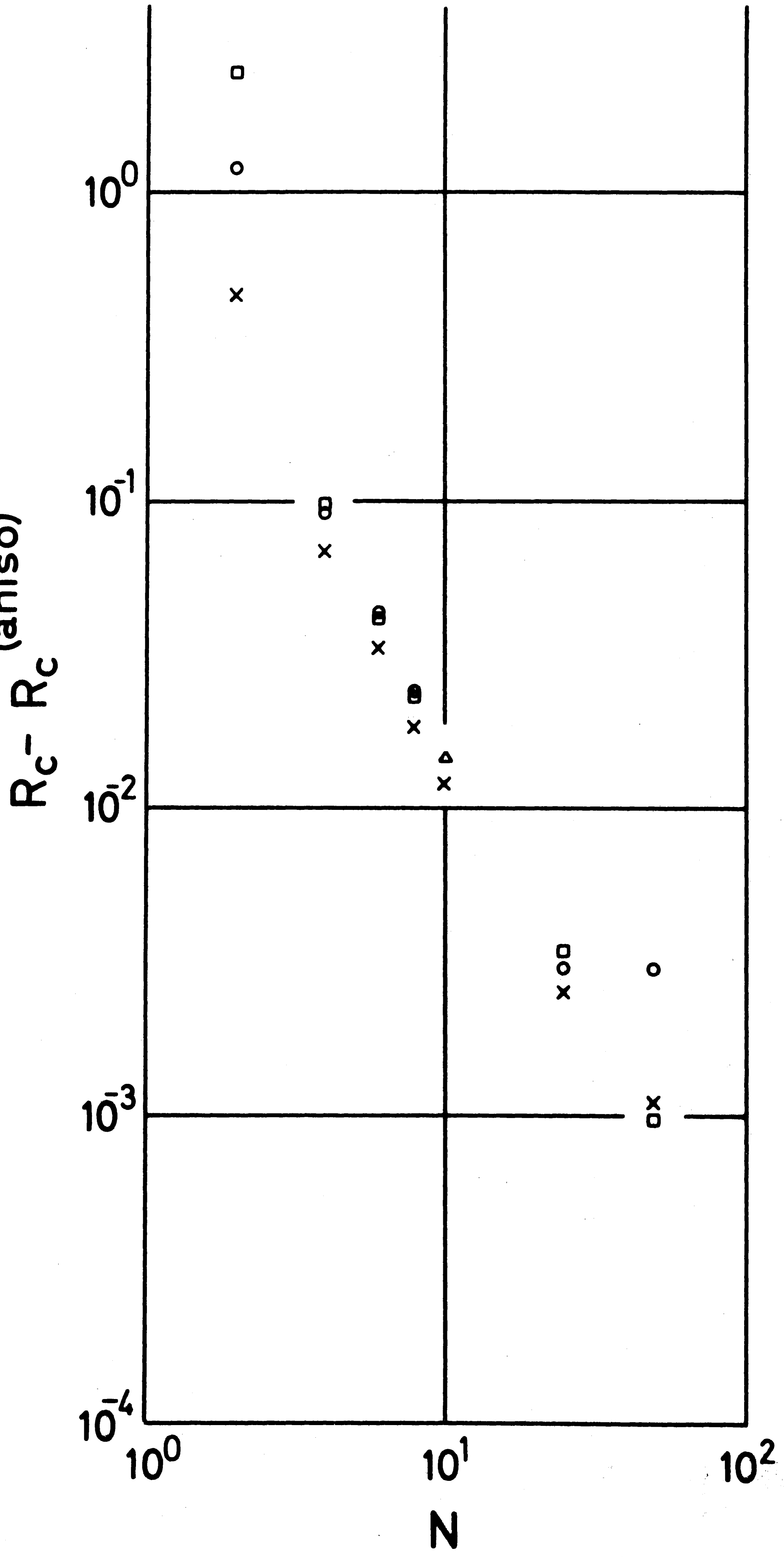

Fig. 3(b).